Macromolecules **2005,** *38,* 1131−1140

Fluorine- and Hydroxyl-Terminated Hyperbranched Poly(phenylquinoxalines) (PPQs) from Copolymerization of Self-Polymerizable AB and AB_2, BA, and BA_2 Monomers

Jong-Beom Baek*,†

School of Chemical Engineering, Chungbuk National University,
Cheongju, Chungbuk 361−763 South Korea

Frank W. Harris*,‡

The Maurice Morton Institute and Department of Polymer Science, The University of Akron,
Akron, Ohio 44325-3909

Received August 12, 2004; Revised Manuscript Received November 8, 2004

ABSTRACT: The **AB** and **AB_2** quinoxaline monomers 2-(4-hydroxyphenyl)-3-phenyl-6-fluoroquinoxaline and 3-(4-hydroxyphenyl)-2-phenyl-6-fluoroquinoxaline (**HPFQ**) and 2,3-bis(4-hydroxyphenyl)-6-fluoroquinoxaline (**BHFQ**) were copolymerized to afford different degree of linear defects in hydroxyl-terminated hyperbranched poly(phenylquinoxalines) (**HT-HPPQ**s). The other set of **BA and BA_2** monomers 2-(4-fluorophenyl)-3-phenyl-6-(4-hydroxyphenoxy)quinoxaline and 2-(4-fluorophenyl)-3-phenyl-6-(4-hydroxyphenoxy)quinoxaline (**FPHPQ**) and 2,3-bis(4-fluorophenyl)-6-(4-hydroxyphenoxy)quinoxaline (**BFHPQ**) were also copolymerized to prepared fluorine-terminated hyperbranched poly(phenylquinoxalines) (**FT-HPPQ**s). On the basis of a MALDI−TOF study of the **HT-HPPQ** sample (**AB_2** 20 mol %), random copolymerization indeed occurred. In the case of **HT-HPPQ**, the properties of polymer such as solubility, solution viscosity, T_g, and polymer degradation temperature were greatly influenced by the number of hydroxyl group on the surface. However, the properties of **FT-HPPQ** were much less influenced by the number of fluorine on the surface. The copolymers of **AB** and **AB_2** were soluble in most of aprotic solvents and phenolic solvents displaying intrinsic viscosities ranged from 0.27 to 1.11 dL/g in *m*-cresol at 30.0 ± 0.1 °C and glass transition temperatures (T_gs) ranged from 239 to 274 °C. Copolymers of **BA** and **BA_2** were also soluble in most of aprotic solvents and phenolic solvents displaying intrinsic viscosities ranged from 1.01 to 1.15 dL/g in *m*-cresol at 30.0 ± 0.1 °C. **HT-HPPQ**s and **FT-HPPQ**s underwent 5% weight losses when subjected to thermal gravimetric analysis ranged from 511 to 568 °C and from 556 to 588 °C in nitrogen atmosphere, respectively. The enhanced thermal stabilities of **FT-HPPQ**s could be attributed to the fluorine terminal groups on the macromolecule surfaces. The melt viscosities of the **HT-HPPQ** sample (AB_2 20 mol %) was greater than 10^7 Pa·s in the lower frequency range determined as a function of frequency sweep on a RMS-800 rheometer at 320 °C. The melt viscosity linearly decreased as the frequency increased. Thus, **HT-HPPQ** containing a 20 mol % AB_2 monomer unit displayed a lower melt viscosity compared to its linear analogue at whole frequency range. However, the relative melt viscosity decrease of hyperbranched PPQ compared to its linear analogue was less than expected due to the formation of possible inter- and intramolecular hydrogen bonding.

Introduction

Hyperbranched poly(phenylquinoxalines) (PPQs) from AB_2 monomers have been previously reported.[1] Their linear analogues are well-known as high performance thermoplastics that have many desirable properties such as melt and solution processabilities, excellent mechanical properties,[2] high glass transition temperatures (T_gs),[2] and promising optical properties with stability.[3] Self-polymerizable PPQ monomer mixtures have been first synthesized in this laboratory and its improved synthetic routes have been reported.[4] It contains both a nucleophilic site and a site activated for nucleophilic substitution by a pyrazine ring. The **AB** monomer mixture, which exists as two isomers, 3-(4-hydroxyphenyl)-2-phenyl-6-fluoroquinoxaline and 2-(4-hydroxyphenyl)-3-phenyl-6-fluoroquinoxaline, has been polymerized in an NMP/toluene mixture to high molecular weight. The **BA** monomer mixture, which also exists as two isomers of 2-(4-fluorophenyl)-3-phenyl-6-(4-hydroxyphenoxy)quinoxaline and 3-(4-fluorophenyl)-2-phenyl-6-(4-hydroxyphenoxy)quinoxaline, has been also polymerized in an NMP/toluene mixture to high molecular weight.[5] The **AB_2** monomer 2,3-bis(4-hydroxyphenyl)quinoxaline has been polymerized in an NMP/toluene mixture to high molecular weight.[1,6] The **BA_2** monomer 2,3-bis(4-fluorophenyl)-6-(4-hydroxyphenoxy)quinoxaline has been also polymerized in an NMP/toluene mixture to high molecular weight (Scheme 1).[1]

Upon further investigation, we discovered that the resulting copolymers display different physical properties such as solubility, solution viscosity, thermal properties, and so on, depending on their degree of surface group interaction. For example, physical properties of hyperbranched PPQs changed depending upon the number of hydroxyl groups as polar surface group. On the other hand, fluorine as less polar surface displayed less change in properties regardless of the number of fluorine atoms on the polymer surface. Although there are a few examples of copolymerization of AB and AB_2 monomers,[7] there are no reported copolymers from both self-polymerizable **AB/AB_2** and **BA_2/BA** monomers to yield a series of rigid hyperbranched polymers with various degrees of linear defects and different number of surface groups, which could significantly influence

---

* Corresponding author.

† Telephone: +82-43-261-2489. Fax: + 82-43-262-2380. E-mail: jbbaek@chungbuk.ac.kr.

‡ Telephone: + 1-330-972-7511. Fax: + 1-330-972-5704. E-mail: fharris@uakron.edu.

10.1021/ma048338r CCC: \$30.25

Scheme 1. Structures of Self-Polymerizable AB, AB_2, BA, and BA_2 Monomers

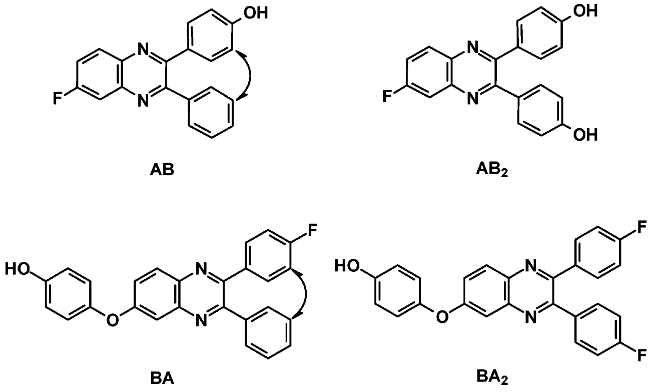

their physical properties, from different feed ratio of monomers.

Thus, the objective of this research was to extend our previous work on hyperbranched PPQ. A series of copolymers by polycondensation of **AB/AB_2** and **BA_2/BA** monomers are to be prepared. The resulting polymers are to be characterized and the properties of polymers are to be compared depending on degree of linear defects and the number of surface groups. Furthermore, physical properties changes are to be speculated by model compounds study.

Experimental Section

Reagents and Solvents. All chemicals, unless otherwise mentioned, were purchased from Aldrich Chemical Inc and were used as received. *N*-Methyl-2-pyrrolidinone (NMP) (Aldrich) was distilled from phosphorus pentoxide under reduced pressure. All other solvents were purchased from Fisher Scientific Inc and were used as received. The intermediates 3,4-diamino-4′-hydroxydiphenyl ether (mp 220−221 °C),[8] 4,4′-difluorobenzil [1,2-bis(4-fluorophenyl)ethanedione] (mp 120−121 °C),[9] and 2,3-bis(4-hydroxyphenyl)quinoxaline (mp 142 and 238 °C) were prepared by modified literature methods.[1,6]

Instrumentation. Infrared (IR) spectra were obtained with an ATI Mattson Genesis Series FT-IR 5000 spectrophotometer. Solid samples were imbedded in KBr disks. Proton and carbon nuclear magnetic resonance (^{1}H NMR and ^{13}C NMR) spectra were obtained at 200 and 50 MHz on a Varian Gemini-200 NMR spectrometer. UV−visible spectra were obtained at Hewlett-Packard 8435 UV−Visible spectrophotometer. Photoluminescence measurement was performed with Shimadzu RF-5301PC Spectrofluorophotometer. Excitation wavelength used was the UV absorption maximum of each sample. Elemental analyses were performed by Galbraith Laboratories, Inc., Knoxville, TN. Melting points (mp) were measured using a Mel-Temp melting point apparatus and are uncorrected. Intrinsic viscosities were determined with a Cannon Ubbelohde No. 100 and 150 viscometers depending on solvent flow time. The solutions were filtered through a 0.45 μm syringe filter prior to the measurement. Flow times were recorded for, *m*-cresol and or methanesulfonic acid (MSA) solutions with polymer concentrations of approximately 0.5−0.1 g/dL at 30.0 ± 0.1 °C. Differential scanning calorimetry (DSC) analyses were performed in nitrogen with a heating rate of 20 °C/min using a du Pont model 2000 thermal analyzer equipped with differential scanning calorimetry cell. Themogravimetric analyses (TGA) were obtained in nitrogen (N_2) atmospheres with a heating rate of 20 °C/min using a TA Hi-Res TGA 2950 themogravimetric analyzer. A Bruker-Franzen Analytik GMBH, MALDI time-of-fight (TOF) mass spectrometer was used to determine masses using a reflection mode. Dithranol and potassium trifluoroacetate were used as UV-absorbing matrix and cationizing salt, respectively. Melt viscosities were obtained on a Rheometrics model RMS-800. The samples for the melt viscosity determinations were compression molded on a 1 in. diameter cylinder mold that was filled with 1−1.5 g of polymer. The mold was placed in a DAKE 100 klb press and heated at 50−100 °C above the polymer T_g under the minimum pressure required for adequate flow. A frequency sweep was used for dynamic measurements. Monte Carlo simulation was carried out by using Discover (version 2.8.0, Biosym Technologies, San Diego, CA). The system was set as completely pure and the same reactivity of monomers.

2,3-Bis(4-octadecyloxyphenyl)-6-fluoroquinoxaline (AB_2-2R). Into a 500 mL, three-necked, round-bottom flask equipped with a magnetic stirrer, a reflux condenser, and a nitrogen inlet were placed **AB_2** monomer, 2,3-bis(4-hydroxyphenyl)-quinoxaline, (10.0 g, 30.1 mmol), 1-bromooctadecane (21.1 g, 63.3 mmol), potassium carbonate (10.0 g, 72.4 mmol), a catalytic amount of 18-crown-6, and acetone (300 mL). The mixture was heated under reflux for 48 h, and 5% hydrochloric acid was slowly poured in. The resulting white precipitate was collected, air-dried, dissolved in warm acetone, and cooled to room temperature to give white flakes (88% yield): mp 87.8 °C (DSC). Anal. Calcd for $C_{56}H_{85}FN_2O_2$: C, 80.33; H, 10.23; N, 3.35. Found: C, 80.14; H, 10.53; N, 3.30. FT-IR (KBr, cm^{-1}): 1346, 1609, 3259. Mass spectrum (*m*/*e*): 837 (M$^+$, 100% relative abundance). ^{1}H NMR ($CDCl_3$) δ 0.85−0.91 (t, 6H, $-CH_3$), 1.28−1.59 (s, 60H, $-CH_2-$), 1.73−1.83 (t, 4H, $-CH_2-$), 3.95−4.01 (t, 4H, $-OCH_2-$), 6.85−6.89 (d, 4H, Ar−*H*), 7.44−7.50 (m, 5H, Ar−*H*), 7.72−7.77 (d, 1H, Ar−*H*), 8.07−8.15 (t, 1H, Ar−*H*). ^{13}C NMR ($CDCl_3$): δ 16.14, 24.71, 28.04, 31.22, 31.37, 31.42, 31.60, 31.97, 32.95, 33.93, 70.08, 114.22, 114.65, 116.34, 121.45, 121.96, 132.87, 133.11, 133.24, 140.21, 143.60, 143.87, 154.48, 154.53, 155.82, 161.79, 161.94, 162.10, 167.09.

2,3-Bis(4-fluorophenyl)-6-(4-methoxyphenoxy)quinoxaline (BA_2-OCH_3). A 500 mL, round-bottom flask equipped with a magnetic stirring bar, a reflux condenser, a Dean−Stark trap, and a nitrogen inlet was charged with 38.0 g (0.154 mol) of 4,4′-difluorobenzil, 38.0 g (0.165 mol) of 3,4-diamino-4′-methoxydiphenyl ether, acetic acid (200 mL), and toluene (100 mL). The reaction mixture was stirred and gently heated at reflux overnight. The water that was generated was removed as a toluene azeotrope. The reaction mixture was then allowed to cool to room temperature and poured into 1 L of a slurry of ice and water containing 50 mL of concentrated hydrochloric acid. The precipitate that formed was collected by suction filtration, washed with water, dried in a vacuum oven at 80 °C, and dissolved in hot toluene or acetic acid. The solution was filtered and then allowed to cool to room temperature to give 65.9 g (97% based on 4,4′-difluorobenzil) of white needles: mp 140−141 °C; mp 144 °C (DSC). Anal. Calcd for $C_{27}H_{18}F_2N_2O_2$: C, 73.63; H, 4.12; N, 6.36. Found: C, 73.70; H, 4.36; N, 6.20. FT-IR (KBr, cm^{-1}): 1229, 1506, 1601, 2922. Mass spectrum (*m*/*e*): 440 (M$^+$, 100% relative abundance). ^{1}H NMR (DMSO-d_6) δ 3.78 (s, 3H, $-OCH_3$), 7.02−7.22 (m, 9H, Ar−*H*), 7.51 (s, 4H, Ar−*H*), 7.58 (d, 1H, Ar−*H*), and 8.12 ppm (d, 1H, Ar−*H*).

General Polymerization Procedure of Copolymers from AB and AB_2 Monomers to Hydroxyl-Terminated Linear and Hyperbranched Polymers. A typical synthesis of hyperbranched PPQ was conducted in a three-necked, round-bottom flask equipped with an overhead stirrer, a Dean−Stark trap with a reflux condenser, and a nitrogen inlet and outlet. The flask was charged with monomer (20 wt % to NMP) and potassium carbonate (20 mol % excess to hydroxyl group). The solids were carefully washed in with the toluene and NMP mixture. The mixture was then heated until the toluene began to reflux. The reaction mixture was maintained at 150−160 °C until water could no longer be observed in the Dean−Stark trap, which typically took about 3−5 h. Upon dehydration, the solution was slowly heated to 180 °C over 1 h under a strong nitrogen flow. The solution was then heated until the NMP began to reflux. Heating at reflux was continued until the solution viscosity drastically increased. This usually took approximately 30−180 min at NMP reflux temperature depending on the ratio of AB/AB_2 monomers. The viscous elastic reaction mixture was diluted with NMP, allowed to cool to room temperature, and poured into large

Scheme 2. Synthesis of HT-HPPQs[a]

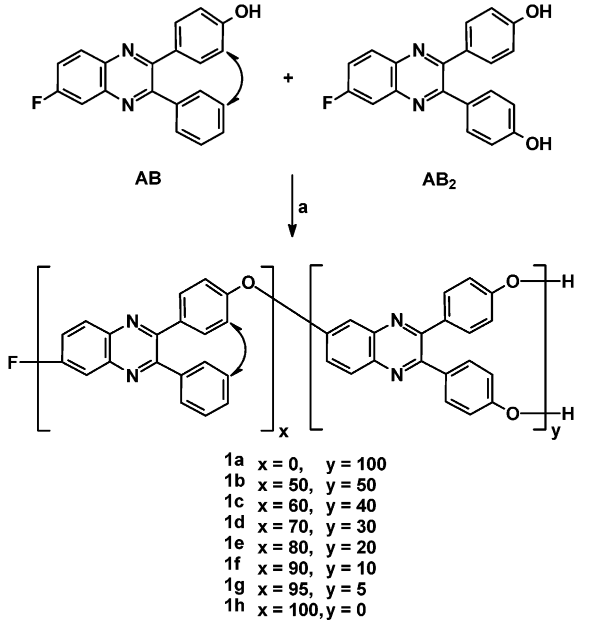

[a] Key: K_2CO_3, NMP/toluene, 150−180−202 °C.

quantity of a methanol/acetic acid (2/1, v/v) mixture. The orange powdery polymer that coagulated was collected by filtration and air-dried overnight. The polymers were dissolved in MSA or NMP again and passed through a pressurized filter to remove any insoluble salts. The filtrate was poured into methanol/water (9/1, v/v) mixture and boiled for several h to remove any trapped salts. The polymers were then Soxhlet extracted with water for 3 days and methanol for 3 days. The polymers were collected and dried at 200 °C over phosphorus pentoxide at reduced pressure (1 mmHg) for approximately 48 h. The yields of polymers were essentially quantitative: **HT-HPPQ** $[\eta] = 0.37−1.29$ dL/g (*m*-cresol or MSA, 30 ± 0.1 °C) and $T_g = 239−308$ °C (DSC).

General Polymerization Procedure of Copolymers from BA and BA$_2$ Monomers to Fluorine-Terminated Linear and Hyperbranched Polymers. The copolymerizations of **AB** and **AB$_2$** monomers were performed the same as any typical synthetic procedure. The viscous reaction mixture was diluted with NMP, allowed to cool to room temperature, and poured into large quantity of a methanol/acetic acid (2/1, v/v) mixture. The white powdery polymer that coagulated was collected by filtration and air-dried overnight. The polymers were dissolved in NMP again and passed through a pressurized filter to remove any insoluble salts. The filtrate was poured into methanol/water (9/1, v/v) mixture and boiled for several h to remove any trapped salts. The polymers were then further Soxhlet extracted with water for 3 days and methanol for 3 days. The polymers were collected and dried at 200 °C over phosphorus pentoxide at reduced pressure (1 mmHg) for approximately 48 h. The yield of polymers were essentially quantitative: **FT-HPPQ** $[\eta] = 0.53−1.13$ dL/g (*m*-cresol, 30 ± 0.1 °C) and $T_g = 206−225$ °C (DSC).

Stock Solution Preparation. To estimate the sample concentration and relative UV-absorption and PL intensity, we prepared stock solutions (1.0×10^{-4} mol/L). Each sample (0.5×10^{-4} mol) was dissolved in a volumetric flask containing 500 mL of THF.

Results and Discussion

Synthesis of Hydroxyl-Terminated Hyperbranched PPQs (HT-HPPQ). The **AB$_2$** monomer was self-polymerized in an NMP/toluene mixture in the presence of potassium carbonate to afford **HT-HPPQ 1a**. **HT-HPPQ 1a** was prepared by the same procedure used for the self-polymerization of the **AB** monomer as shown in Scheme 2.[4]

Table 1. Properties of Linear and Hydroxyl-Terminated Hyperbranched PPQs

	composition				TGA	
no.	AB (wt %)	AB$_2$ (wt %)	$[\eta]$[a] (dL/g)	T_g[b] (°C)	$T_{d5\%}$[c] in N_2 (°C)	char % at 800 °C
1a	0	100	0.60[d]	308	511	70
1b	50	50	0.68	274	559	65
1c	60	40	0.37	263	568	69
1d	70	30	0.31	255	542	69
1e	80	20	0.27	239	556	68
1f	90	10	0.56	247	556	64
1g	95	5	1.11	254	549	58
1h	100	0	1.29	256	584	66

[a] Intrinsic viscosity measured in *m*-cresol at 30.0 ± 0.1 °C. [b] Inflection in baseline on DSC thermogram obtained in N_2 with a heating rate of 20 °C/min. [c] Temperature at which 5% weight loss occurred on TGA thermogram obtained with a heating rate of 20 °C/min. [d] Intrinsic viscosity measured in methanesulfonic acid at 30.0 ± 0.1 °C.

The dark elastic jellylike polymer solutions were poured into a large excess of methanol containing 5% hydrochloric acid to precipitate the product. The polymers were carefully worked-up following the procedure described in experimental part. The yields of polymers were essentially quantitative. The excellent solubility of linear poly(phenylquinoxalines) (PPQs) have been proven by the interesting thermal behaviors of self-polymerizable **AB** quinoxaline monomers had been reported.[4c,4e] This behavior is due to two phenyl rings at the 2- and 3-positions of the 2,3-diphenylquinoxaline ring being 44° out of plane; thus chain packing is difficult, resulting in a very slow rate of crystallization from the melt. The structure of isomeric repeating unit provide good solubility of resulting linear poly(phenylquinoxaline).[4] However, the residual solvent free polymer **HT-HPPQ 1a** could only be dissolved in organic acids such as methanesulfonic acid (MSA) and sulfuric acid at room temperature. The intrinsic viscosity was able to be determined from the solution in MSA to give 0.60 dL/g (30 ± 0.1 °C).[1] The poor solubility could be originated by existing large number of surface hydroxyl groups that could form strong inter- and intramolecular hydrogen bonding. Thus, the T_g of **HT-HPPQ 1a** was 308 °C, which was approximately 52 °C higher than that of the linear PPQ **1h** (256 °C, see Table 1).

HPPQs from the Copolymerization of AB and AB$_2$ Monomers. In general, the hyperbranched polymer is well-known to be highly solubile compared to its linear analogue.[10] Since irregular size of globular molecular shape in hyperbranched polymer prevents molecular packing and cavities in the structure allows the penetration of solvent. The unusual limited solubility of **HT-HPPQ 1a** obtained from the **AB$_2$** monomer compared to its linear analogue[4] could be due to the large number of hydroxyl groups on the hyperbranched macromolecules. It is worthwhile to attempt to change the number of hydroxyl groups at the chain ends and, thereby, increase the solubility. Thus, several copolymerizations of the **AB** and **AB$_2$** monomers were carried out to afford a series of **HT-HPPQ** copolymers **1b**−**1g** (Scheme 2). The copolymerizations were carried out by the general procedure for the self-polymerization of the **AB** monomer.[4] High molecular weight copolymers were obtained within 3 h as judged by the dramatic increases in the solution viscosities. **HT-HPPQ**s **1b**−**1g** after complete workup and dryness were soluble in polar aprotic solvents such as *N*-methyl-2-pyrrolidinone (NMP), *N,N'*-dimethylformamide (DMF), *N,N'*-dimethylacetamide (DMAc), dimethyl sulfoxide (DMSO), etc. The

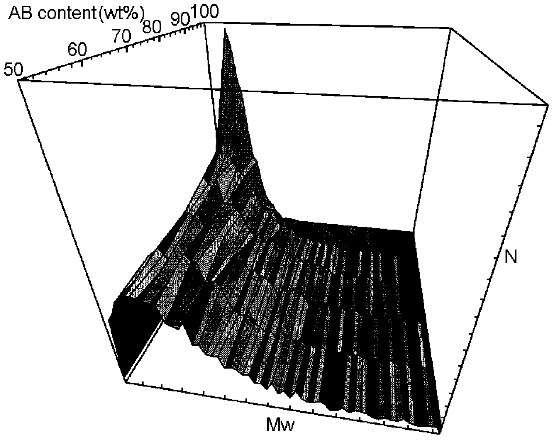

Figure 1. Calculated molecular weight distributions of linear and hyperbranched PPQs [Monte Carlo simulation with a total number of 50 000 (**AB$_2$** + **AB**)].

intrinsic viscosities of **HT-HPPQ**s **1b**−**1g** ranged from 0.27 to 1.11 dL/g (*m*-cresol, 30 ± 0.1 °C) and T_gs were 239−274 °C. Thus, it could be stated that the limited solubility of **HT-HPPQ 1a** originated from a large number of polar hydroxyl groups, which could form strong inter- and intramolecular hydrogen bonding.

Monte Carlo Simulation. Assuming that the purities of monomers were 100% and the reactivity of the functional groups on the monomers were the same. A total number of 50 000 **AB** and **AB$_2$** monomers with different ratio were randomly reacted. The theoretical molecular weight distributions of the hyperbranched PPQs as a function of **AB$_2$** content were calculated using a Monte Carlo simulation. The results are shown in Figure 1. As the **AB$_2$** content increased, the molecular weight distribution (MWD) broadened. The reaction time was shorter as the **AB$_2$** content increased to reach 100 000 g/mol.

MALDI—TOF Mass Analysis of Copolymer 1e. MALDI−TOF analysis of homopolymer **FT-HPPQ 2a** has been previously reported.[1] The copolymer of **HT-HPPQ 1e**, which contained 20 mol % of the AB$_2$ component, has been studied (Figure 2, parts a and b). A series of signals, which were 296 Da apart, was observed to 8000 Da. The oligomers ($n = x + y = 3−27$) were randomly formed by the reaction of **AB** and **AB$_2$** monomers. Each set of peaks, which was separated 16 Da apart, provided the ratio of **AB** and **AB$_2$** components in the macromolecules. According to their *m*/*z* values from Figure 2b and Table 2 where it is zoomed in the range of *m*/*z* = 2000−2800, the peaks marked ***a*** appeared to be macrocyclic oligomers (*m*/*z* = 2076.3 corresponding to $x = 7$, *m*/*z* = 2372.8 corresponding to $x = 8$, and *m*/*z* = 2668.5 corresponding to $x = 9$) formed by **AB** monomers (Scheme 2 and Table 2). The peaks marked ***b*** appeared 16 Da higher than those marked ***a*** at 2091.9, 2788.2, and 2684.3 and represent an oxygen atom count. Thus, this series of macrocyclic oligomers contained an **AB$_2$** component ($y = 1$). The peaks marked ***c*** appeared 18 Da higher than those marked ***b*** at 2110.9, 2406.1, and 2701.6. It could be the oligomers containing an **AB$_2$** ($m = 1$) and fluorine atom (F) as a focal point. The peaks marked ***d*** appeared 16 Da higher than those marked ***c*** at 2126.4, 2422.7, and 2718.7 and are most likely due to two **AB$_2$** components ($m = 2$) and F. The peaks marked ***e*** and ***f*** appeared 16 and 32 higher than ***d*** and presumably correspond to three **AB$_2$** components ($m = 3$) plus F and four **AB$_2$** components ($m = 4$) plus F. In summary, The **AB** and **AB$_2$** monomers displayed very similar reactivity. Therefore, random copolymers were mainly observed.

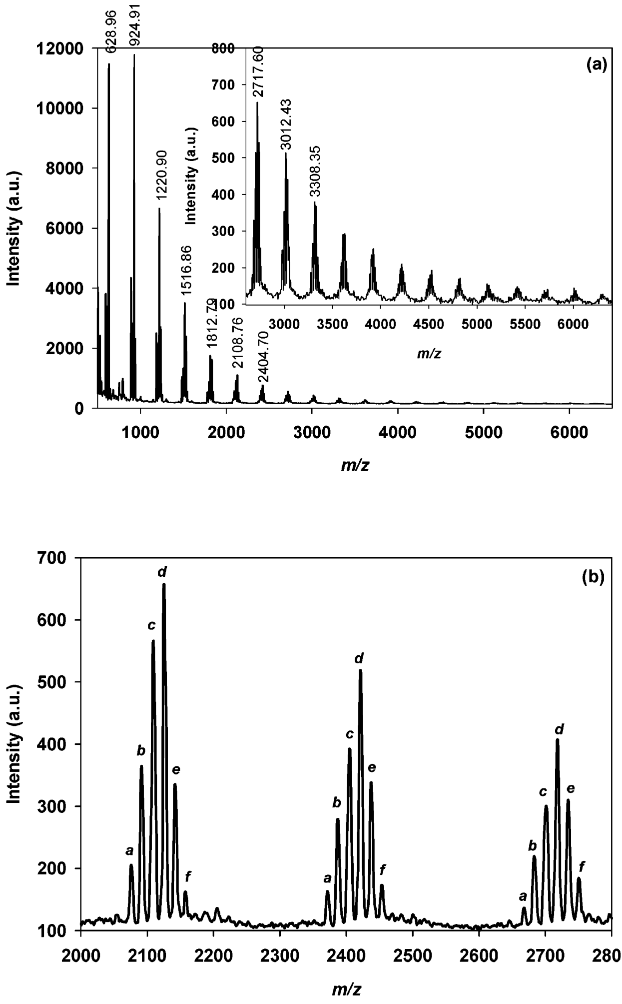

Figure 2. MALDI−TOF mass spectrum of HT-HPPQ **1e** (**AB$_2$** 20 mol %): (a) full scale and expanded into 2600 to 6400 Da; (b) expanded into 2000 to 2800 Da.

Table 2. MALDI−TOF Analysis

entry	*x*	*y*	*m*/*z*	*m*/*z*	*m*/*z*
a	7−9	0	2076.3	2372.8	2668.5
b	6−8	1	2091.9	2388.2	2684.3
c	6−8	1 (+F)	2110.2	2406.1	2701.6
d	5−7	2 (+F)	2126.4	2422.7	2718.7
e	4−6	3 (+F)	2142.5	2438.6	2734.8
f	3−5	4 (+F)	2158.3	2454.7	2750.9

Synthesis of Fluorine-Terminated Hyperbranched PPQs (FT-HPPQ). The **BA$_2$** monomer was self-polymerized in an NMP/toluene mixture in the presence of potassium carbonate. The polymerization was carried out by the same procedure used for the self-polymerization of the **AB** monomer as shown in Scheme 3.[5] The resulting white **FT-HPPQ 2a** had an intrinsic viscosity of 1.13 dL/g (*m*-cresol at 30.0 ± 1 °C) and a T_g of 225 °C. We have reported the characteristic solution behavior of homopolymer **2a**, which was soluble in THF and most aprotic solvents and was analyzed with GPC using a refractive index detector, a light scattering detector, and a viscosity detector.[1]

Hyperbranched polymers are known to be molecular bearing, which can reduce the melt viscosity of thermoplastic.[11] **FT-HPPQ 2a** has been tested as potential processing aids by blending with commercial polycar-

Scheme 3. Synthesis of FT-HPPQs[a]

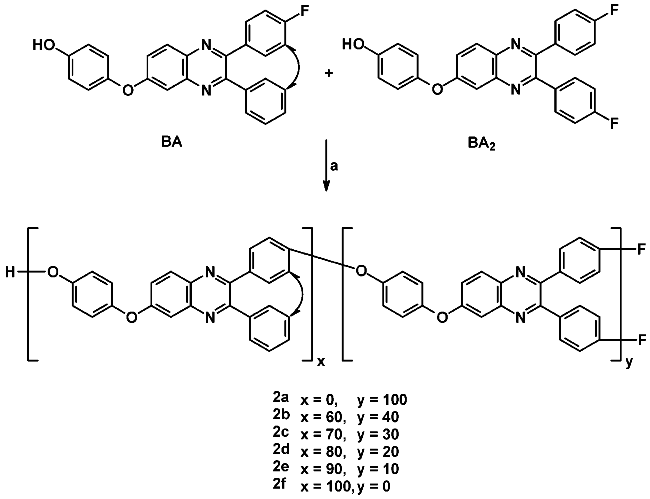

[a] Key: K_2CO_3, NMP/toluene, 150−180−202 °C.

Table 3. Properties of Linear and Fluorine-Terminated Hyperbranched PPQs

	composition				TGA[c]	
no.	**BA** (wt %)	**BA_2** (wt %)	[η][a] (dL/g)	T_g[b] (°C)	$T_{d5\%}$ in N_2 (°C)	char % at 800 °C
2a	0	100	1.13	225	575	68
2b	60	40	1.06	217	582	63
2c	70	30	1.07	221	588	64
2d	80	20	1.01	217	581	63
2e	90	10	1.15	206	556	59
2f	100	0	0.53	220	550	59

[a] Intrinsic viscosity measured in *m*-cresol at 30.0 ± 0.1 °C. [b] Inflection in baseline on DSC thermogram obtained in N_2 with a heating rate of 20 °C/min. [c] Temperature at which 5% weight loss occurred on TGA thermogram obtained with a heating rate of 20 °C/min.

bonate (PC). **FT-HPPQ 2a** indeed linearly lowered melt viscosity of PC, which does not have a shear thinning property in melt.[1]

HPPQs from the Copolymerization of BA and BA_2 Monomers. Various weight ratios of the **BA** monomer and **BA_2** monomer were copolymerized in an NMP/toluene mixture in the presence of potassium carbonate to yield hyperbranched PPQ copolymers **2b**−**2e** (Table 3). The polymerizations were carried out by the same procedure used for the self-polymerization **AB** monomer as shown in Scheme 3.[4]

High molecular weight copolymers were also obtained within 2 h as judged by the dramatic increases in the solution viscosities. **FT-HPPQ**s **2b**−**2e**, after complete workup and dryness, were soluble in polar aprotic solvents such as *N*-methyl-2-pyrrolidinone (NMP), *N,N′*-dimethylformamide (DMF), *N,N′*-dimethylacetamide (DMAc), dimethyl sulfoxide (DMSO), and so on. The intrinsic viscosities of **HT-HPPQ**s **2b-2e** ranged from 1.01 to 1.15 dL/g (*m*-cresol, 30 ± 0.1 °C) and T_gs were 206−221 °C.

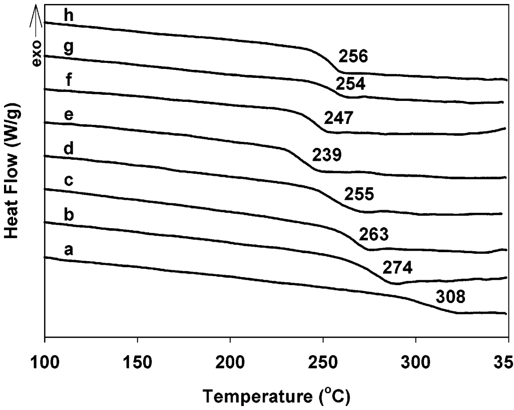

Figure 3. DSC thermograms of **HT-HPPQ**s with heating rate of 20 °C/min: (a) **1a**, (b) **1b**, (c) **1c**, (d) **1d**, (e) **1e**, (f) **1f**. (g) **1g**, and (h) **1h**.

Thermal Properties of HT-HPPQs. The physical properties of dendritic macromolecules such as dendrimers and hyperbranched polymers are significantly influenced by the nature of their surface functional groups. The glass transition temperature (T_g) of dendritic macromolecules with identical interiors but different surface groups could be one method to observe changing properties.[12] For example, the T_g of hyperbranched polyphenylene with different terminal groups can be altered by more than 100 °C.[12e] The different surface groups also influence polarity, solubility, and in many cases the dimension and the shape of the dendritic macromolecules.[13]

DSC thermograms were obtained on powder samples after they had been heated to 350 °C and air-cooled to ambient temperature. The T_g was taken as the midpoint of the maximum baseline shift. As shown in Table 1 and Figure 3, the linear PPQ displayed a T_g as high as 256 °C ([η] = 1.29 dL/g).

HT-HPPQ 1a obtained from **AB_2** monomer displayed a T_g of 308 °C.[1] This T_g is approximately 52 °C higher than that of the linear analogue **1h**. It is postulated that this is due to strong inter- and intramolecular hydrogen bonding between surface hydroxyl groups. The **HT-HPPQ** copolymers displayed T_gs in the range of 239 to 274 °C depending on their **AB_2** unit content, which determined the number of hydroxyl groups. As the **AB_2** content increased up to 20%, the intrinsic viscosities and T_gs of the hyperbranched copolymers decreased. It was postulated that the viscosity decrease and the T_g decrease in lower contents of **AB_2** monomer were due to the decrease in branch length. On the other hand, as the **AB_2** content increased from 30% to 50%, both the viscosities and the T_gs of the hyperbranched copolymers increased. It is postulated that the **AB_2** content increased and the number of hydroxyl group on the macromolecule surface increased, hydrogen bonding between the chain ends became significant resulting in an increase in T_g and affected intrinsic viscosity. The thermal properties of the **HT-HPPQ**s are summarized in Table 1. The temperature at which a 5% weight loss occurred when the polymers were subjected to TGA in N_2 ranged from 511 to 584 °C. As the number of hydroxyl groups at the chain ends increased, the thermal stabilities of polymers generally decreased. The linear PPQ **1h** having the minimum number of hydroxyl groups displayed the highest degradation temperature at 584 °C. The char yields (58−70%) at 800 °C were for all the **HT-HPPQ**s.

Thermal Properties of FT-HPPQs. DSC thermograms were obtained on the copolymers after they had been heated to 350 °C and air-cooled to ambient temperature (Figure 4). For comparison purposes, the thermograms of the linear PPQ **2f** and the hyperbranched PPQ **2a** are included in Figure 4. As stated before, the T_gs of these polymers are 223 and 225 °C, respectively. All the T_gs and viscosities of the fluorine-terminated PPQ copolymers were similar regardless of their **BA_2** content. These results are dramatically different from those obtained with **HT-HPPQ 2a** copoly-

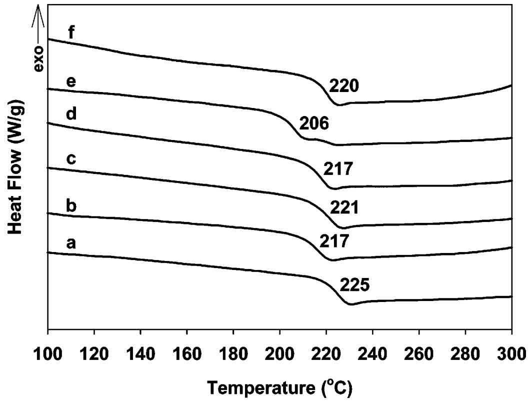

Figure 4. DSC thermograms of **FT-HPPQ**s with heating rate of 20 °C/min: (a) **2a**, (b) **2b**, (c) **2c**, (d) **2d**, (e) **2e**, and (f) **2f**.

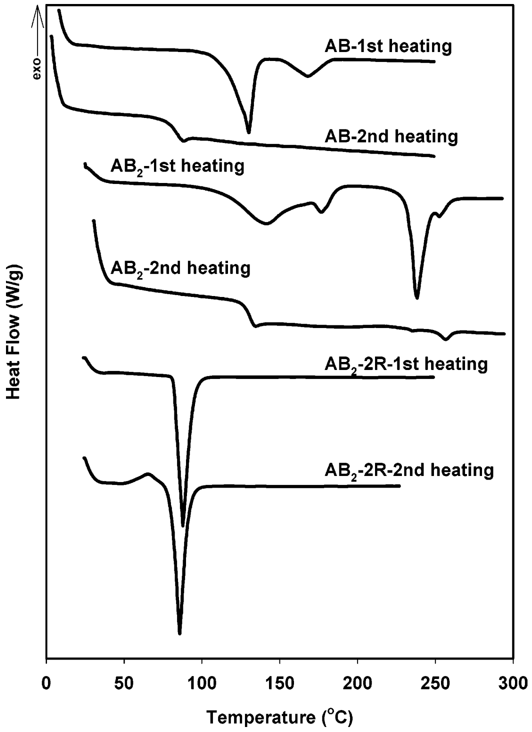

Figure 5. DSC thermograms of **AB**, **AB$_2$**, and **AB$_2$-2R** with heating rate of 20 °C/min.

Table 4. UV Absorption, Emission, and Thermal Properties of Quinoxaline Compounds

			DSC[c]				
monomer	λ_{ab}[a] (nm)	λ_{em}[b] (nm)	T_g (°C)	T_{m1} (°C)	ΔH_{f1} (J/g)	T_{m2} (°C)	ΔH_{f2} (J/g)
AB	367	441	84.4	130.4	54.5	165.8	7.1
AB$_2$	376	441	131.0	141.8	129.3	238.3	92.0
AB$_2$-2R	373	434	ND	87.8	142.8	ND	ND
BA	366	412	89.8	238.1	120.9	ND	ND
BA$_2$	369	416	90.4	223.2	113.5	ND	ND
BA$_2$-OCH$_3$	369	426	48.0	143.8	96.4	ND	ND

[a] Obtained in 10^{-4} mol in THF solution. [b] Obtained in 10^{-4} mol in THF solution with excited at absorption maximum. [c] Obtained in N_2 with a heating rate of 20 °C/min.

mers. This is again postulated to be due to the charge repulsion of fluorine atoms at each chain end in the **FT-HPPQ 2a**. The properties of **FT-HPPQ**s **2b**−**2e** copolymers are summarized in Table 3.

The temperatures at which the **FT-HPPQ**s **2a**−**2e** underwent a 5% weight loss when subjected to TGA ranged from 550 to 588 °C, which were higher than those of **HT-HPPQ**s. Although one more aromatic ether linkage was incorporated into each repeating unit, the thermal stabilities of the **FT-HPPQ**s were better than those of the **HT-HPPQ**s. This is because thermal degradation is heavily dependent on the surface functional groups at the chain ends.

Thermal Properties of Monomers and Model Compounds. To provide evidence of the assumption that hydrogen bonding would be the main reason for a significant increase in the T_g of **HT-HPPQ 1a** compared to its linear analogue **1h**, the DSC thermograms of **AB** (single hydroxyl group) monomer mixture and **AB$_2$** (two hydroxyl groups) monomer are compared in Figure 5 and Table 4. From the first heating run, the **AB** monomer mixture exhibited two melting endotherm at peak maxima at 130.4 °C and the second minor endotherm at peak maximum at 165.8 °C. Even though there is no isomeric mixture in **AB$_2$** monomer, two major melting peaks were monitored at the peak maximum at 141.8 °C and 238.3 °C from the first heating run. Two minor melting peaks, which postulated to be originated from dissociation of hydrogen bonding, were at 177.2 °C (ΔH_{diss1} = 22.3J/g) and 252.5 °C (ΔH_{diss2} = 11.7 J/g). In comparison of the T_gs between **AB** and **AB$_2$** in the second heating runs, T_g (131.0 °C) of **AB$_2$** monomer was 46.6 °C higher than that of **AB** (84.4 °C) monomer mixture. This different on T_gs of **AB** and **AB$_2$** monomers could be an evidence to support T_g increase in **HT-HPPQ 1a** originated by hydrogen bonding. Dissociation of hydrogen bonding of **AB$_2$** monomer could be monitored even in the second heating run at 256.6 °C (ΔH_{diss} = 1.6 J/g). To prevent hydrogen bonding, flexible alkyl chains were introduced on **AB$_2$** to afford **AB$_2$-2R** monomer as shown in Scheme 4, the crystallization rate was fast enough to display very similar thermal behaviors at each cycle. The melting temperatures of **AB$_2$-2R** were at 87.8 °C and 85.8 °C in both the first and the second heating runs with recrystallization temperature at 65.5 °C (ΔH_{exo} = 10.3J/g) without detectable T_g (Figure 5) by DSC.

In the case of monomers **BA** and **BA$_2$**, the DSC thermograms of **BA** (single hydroxyl group) monomer mixture and **BA$_2$** (single hydroxyl group) monomer are compared in Figure 6 and Table 4. From the first heating run, the **BA** monomer mixture exhibited single melting endotherm at peak maximum at 238.1 °C with left shoulder, which may be originated from crystals of isomeric mixture. For the **BA$_2$** monomer, single melting peaks were monitored at peak maximal at 223.2 °C from the first heating run. In comparison of the T_gs between **BA** and **BA$_2$** in the second heating run, T_g (90.4 °C) of **BA$_2$** monomer was similar to that (89.8 °C) of **BA** monomer mixture. The similarity in T_gs as well as T_ms of **BA** and **BA$_2$** monomers could be an evidence to support similar T_g in **FT-HPPQ 2a**. When hydroxyl groups were protected to eliminate hydrogen bonding by methyl group on **BA$_2$** to afford **BA$_2$-OCH$_3$** monomer as shown in Scheme 4, the melting temperature significantly dropped to 143.8 °C in the first run and displayed lowered T_g at 48.0 °C in the second heating run. There was no crystal melting in the second run like **AB$_2$-2R**, since the crystallization rate was not fast enough with the short methyl substitute.

This indicates that T_gs as well as T_ms of quinoxaline monomers may vary depending on the degree and presence of hydrogen bonding in the molecules. Multiple morphisms in some of the quinoxaline monomers are believed to be caused by monomers that are trapped in

Scheme 4. Synthesis of 2,3-Bis(4-octadecyloxyphenyl)-6-fluoroquinoxaline (AB_2-2R) and 2,3-Bis(4-fluorophenyl)-6-(4-methoxyphenoxy)quinoxaline (B_2A-OCH_3)[a,b]

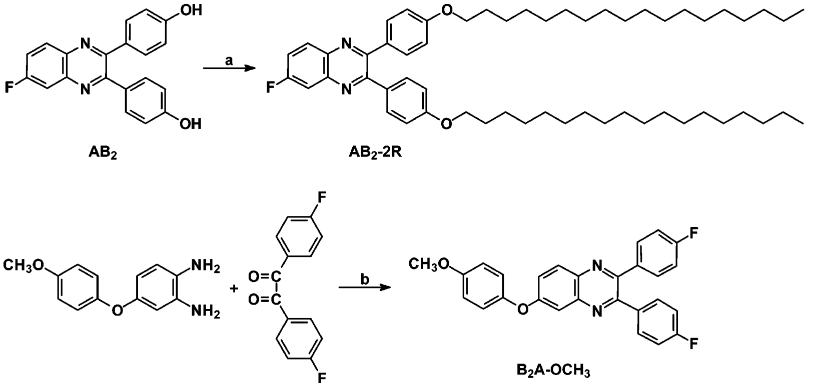

[a] Key: $C_{18}H_{37}Br$, K_2CO_3, acetone, reflux. [b]Key: acetic acid, reflux.

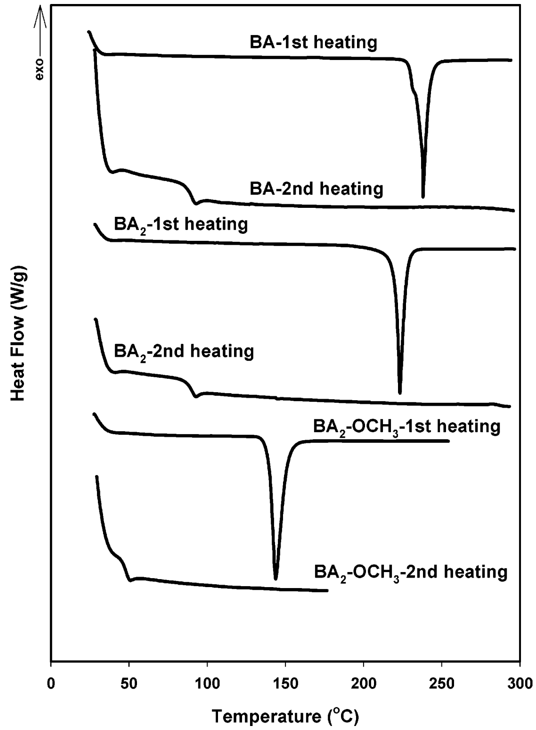

Figure 6. DSC thermograms of **BA**, $\mathbf{BA_2}$, and $\mathbf{BA_2}$**-**$\mathbf{OCH_3}$ with heating rate of 20 °C/min.

their amorphous forms after melt. In most cases of quinoxaline monomers, only solvent-induced crystallizations were possible for the monomer mixtures as demonstrated by $\mathbf{AB_2}$**-2R**, on which long alkyl chains act as flexible spacers to allow the mobility of recrystallization. The same DSC thermograms could be obtained after recrystallization of molten monomer mixtures from proper solvents. Furthermore, the thermal studies of monomers made it possible to predict relative the thermal properties of **HPPQ**s.

UV Absorption and Emission Properties. Quinoxaline compounds are well-known to be photoluminescent (PL) and electroluminescent (EL) materials, because they displayed surprisingly unaltered from luminescent properties without electron-transporting layer and long-term stability.[14a] In practice, 2,3-diphenylquinoxaline compounds poses excellent solubility,[14b–i] since the 2- and 3-position phenyl rings are 44° out of plane to quinoxaline ring, which consisted of a fused aromatic heterocyclic ring and two additional aromatic rings; they are disrupting the molecular packing and are conjugated enough to be optically active.[1,14c]

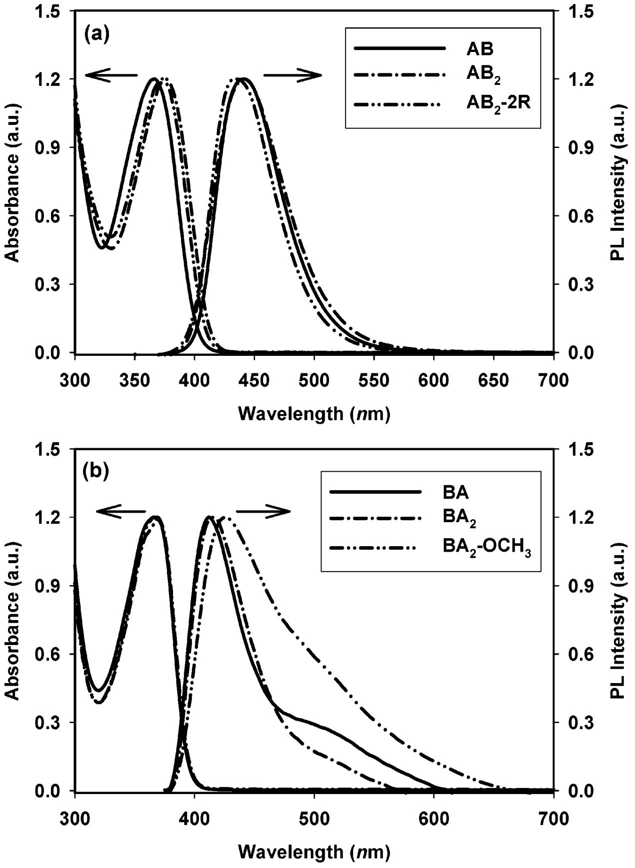

Figure 7. UV-absorption and emission spectra in THF solutions (1.0×10^{-4} mol/L).

Stock solutions (1.0×10^{-4} mol/L) of each sample were prepared in THF and UV absorption and emission were obtained. The absorption maxima of **AB**, $\mathbf{AB_2}$, and $\mathbf{AB_2}$**-2R** are 367, 376, and 373 nm in that order (Figure 7a and Table 4). Additional hydroxyl group on $\mathbf{AB_2}$ compared to **AB** causes a 9 nm red-shifted absorption maximum. When hydroxyl groups on $\mathbf{AB_2}$ were replaced by $\mathbf{AB_2}$**-2R** ($R = C_{18}H_{37}$), the absorption maximum was 3 nm blue-shifted. Thus, the effective conjugate length at ground state of $\mathbf{AB_2}$ is the longest among them, since this molecule can form a stable dimer in solution as depicted in Figure 8. The dihedral angle of 2- and 3-phenyl rings to the quinoxaline ring was reduced from 44 to 36°, which might result in an increasing effective

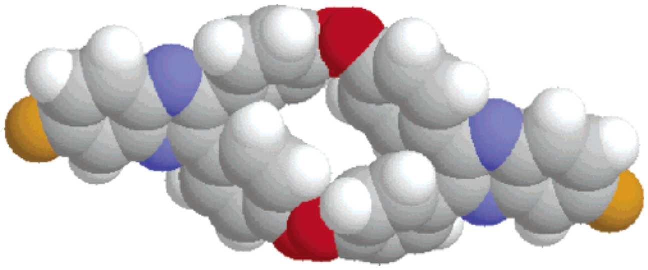

Figure 8. Space filling model after energy minimization of **AB$_2$** dimer formed by hydrogen bonding (dihedral angles of 2- and 3-phenyl rings to the quinoxaline ring are 36°).

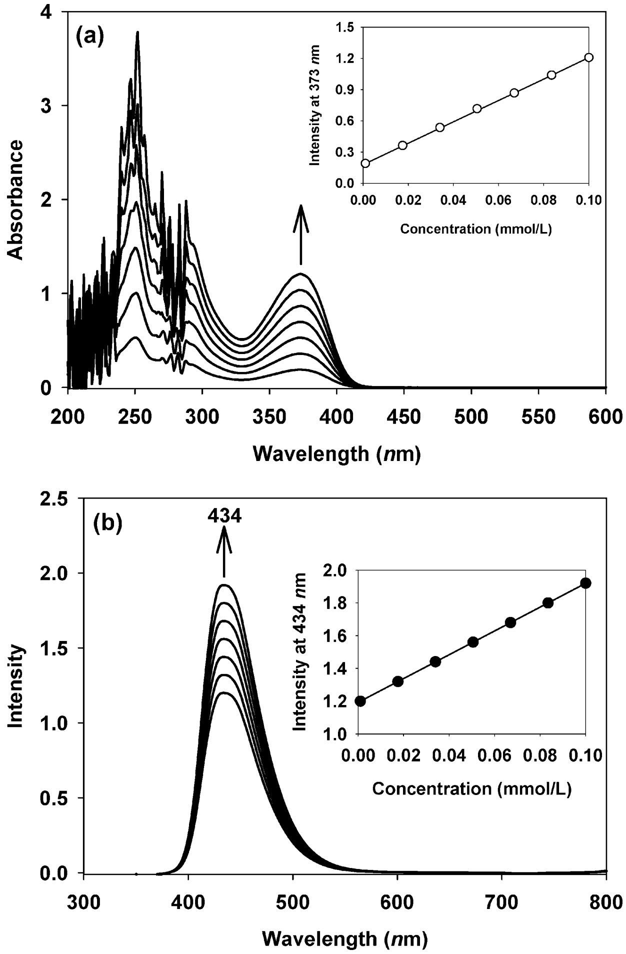

Figure 9. UV-absorption and emission spectra of **AB$_2$-2R** in THF solutions.

degree of conjugation, and thus the absorption maximum red-shifted. The emission maxima for the monomer **AB**, **AB$_2$**, and **AB$_2$-2R** are 441, 441, and 434 nm, respectively (Figure 7a and Table 4). **AB** and **AB$_2$** displayed the same emission maxima indicating energy band gaps are almost identical. However, **AB$_2$-2R** has a slightly smaller band gap. This could be simply because bulky octyl groups isolate the quinoxaline moiety, and there is no interaction between quinoxaline moieties possible.

The absorption maxima of **BA**, **BA$_2$**, and **BA$_2$-OCH$_3$** are 366, 369, and 369 nm in that order (Figure 7b and Table 4). There was no significant shift on absorption maxima depending on the number of fluorine atoms. Additional fluorine group on **BA$_2$** compared to **BA** causes merely a 3 nm red-shifted absorption maximum. Not like **AB** to **AB$_2$**, when hydroxyl groups on **BA$_2$** were replaced with **BA$_2$-OCH$_3$**, the absorption maximum was not changed. This is because the hydroxyl group located a phenyloxy away from the quinoxaline ring does not influence the effective conjugation length at ground state of **BA$_2$-OCH$_3$** as depicted in Figure 7b. The emission maxima for the monomers **BA**, **BA$_2$**, and **BA$_2$-OCH$_3$** are 412, 416, and 426 nm, respectively (Figure 7b and Table 4). The emission maxima of **BA** and **BA$_2$** displayed the close values indicating that additional fluorine atom does not affect energy band gap. However, the emission maximum of **BA$_2$-OCH$_3$** was 14−16 nm red-shifted, and the right shoulder of the emission peak was much larger compared to those of **BA** and **BA$_2$**, suggesting there were higher chances of excimer formation among these molecules in THF solution. To test this phenomenon, stock solutions were diluted with pure THF, and both UV-absorption and emission scans were run as a function of concentration. Interestingly, the model compounds **AB$_2$-2R** and **BA$_2$-OCH$_3$** showed that the intensities of UV-absorption were stronger as concentration increased (Figure 9a and Figure 10a). The plots of intensities at absorption maxima vs concentration followed linear dependence for both cases (small figures in Figure 9a and Figure 10a). However, emission behaviors of **AB$_2$-2R** and **BA$_2$-OCH$_3$** were completely reversed (Figure 9b and Figure 10b). The emission intensity of **AB$_2$-2R** linearly increased as concentration increased (Figure 9b), whereas that of **BA$_2$-OCH$_3$** was linearly decreased (Figure 10b). In summary, the polarity of materials greatly influence the thermal properties as well as optical properties.

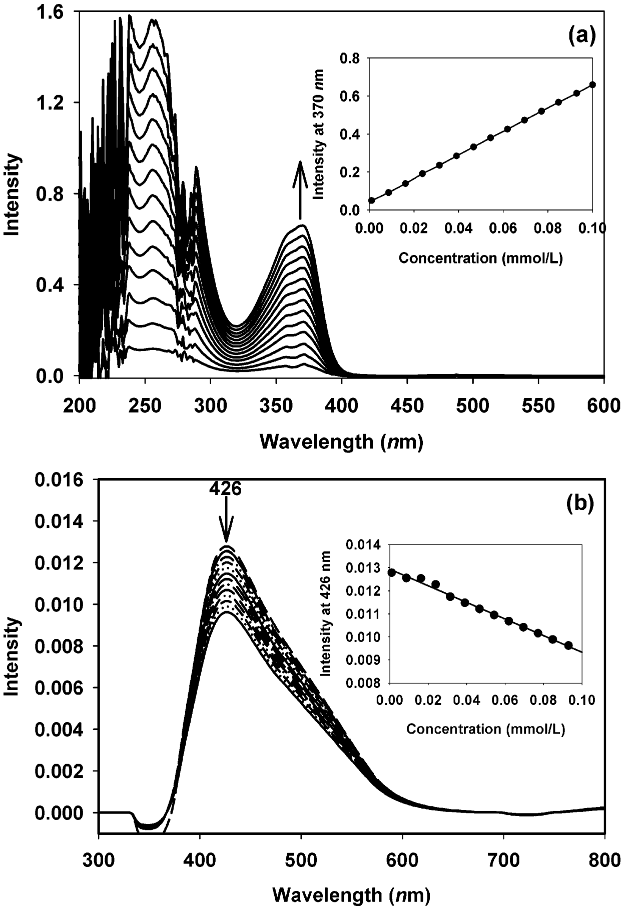

Figure 10. UV-absorption and emission spectra of **BA$_2$-OCH$_3$** in THF solutions.

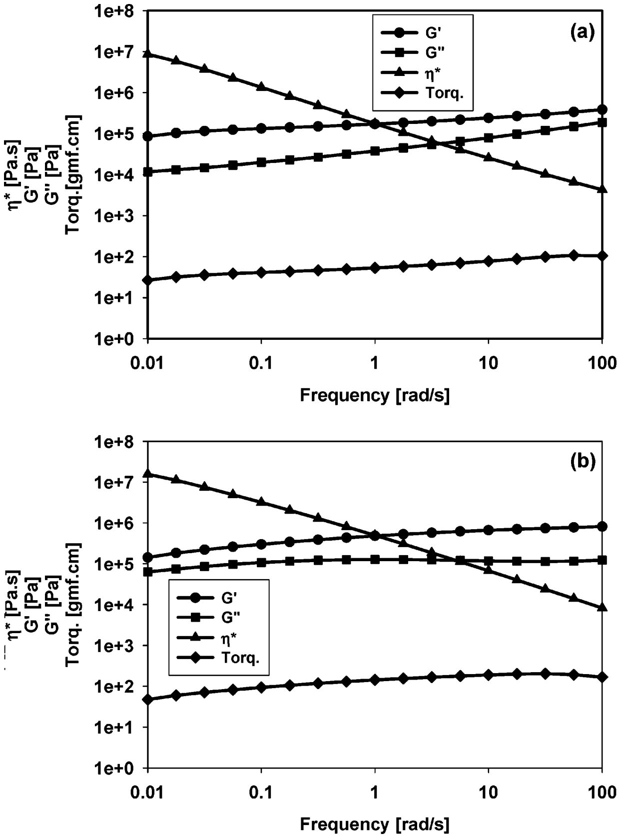

Figure 11. Melt viscosities of (a) linear reference PPQ (IV = 1.29 dL/g) and (b) HT-HPPQ **1e** (AB$_2$ 20 mol %) as a function of frequency at 320 °C with 1% strain.

Melt Viscosity. The melt viscosities of a sample of the hyperbranched **HT-HPPQ 1e** with intrinsic viscosities of 0.27 dL/g were determined as a function of frequency on a RMS-800 rheometer at 320 °C with 1% strain (Figure 11a). The melt viscosities of **HT-HPPQ 1e** were approximately 10^7 Pa•s, which was lower than that of linear analogue **1h**, in the all frequency range from 10^{-2} to 10^2. The melt viscosity was linearly decreased as the frequency increased. Thus, hyperbranched PPQ **1e** displayed a better shear thinning effect. This is a great advantage for a processing aid. However, the melt viscosity decrease of **HT-HPPQ 1e** compared to the linear analogue (Figure 10b) was less than expected. It is postulated that this was due to the presence of the large number of hydroxyl groups at the chain ends. Intermolecular hydrogen bonding can be formed in the melt. Thus, the effect of the change in molecular shape was counterbalanced by the effect of hydrogen bonding.

Conclusion

Hyperbranched copolymers of **HT-HPPQ**s, and **FT-HPPQ**s were prepared from self-polymerizable **AB** and **AB$_2$** monomers and **BA** and **BA$_2$** monomers, respectively. In the cases of HT-PPQs, solubility, solution viscosities, T_gs, and thermal stabilities varied depending on **AB$_2$** unit contents in the **HT-HPPQ** copolymers. The number of hydroxyl groups which could form inter- and intramolecular hydrogen bonding is supposed to be the main reason for altered solubility, T_gs, and degradation temperatures. From the thermal studies on monomers, present hydrogen bonding was supporting evidence of T_gs changes in **HT-HPPQ**. The T_g of **AB$_2$** monomer was about 35 °C higher than that of the **AB** monomer. On the other hand, solubility, T_gs, and solution viscosities of **FT-HPPQ**s were not much affected by fluorine surface groups. However, the thermal stabilities were heavily affected by kinds of surface groups.

The melt viscosities of sample of the **HT-HPPQ** was started approximately from 10^7 Pa•s at 10^{-2} rad/s to below 10^4 Pa•s at10^2 as a function of frequency on a RMS-800 rheometer. Thus, hyperbranched PPQ did display a shear thinning effect. However, the melt viscosity decrease of hyperbranched PPQ compared to linear analogue was less than expected due to the formation of hydrogen bonding in the melt.

Acknowledgment. This work was supported in part by NASA-Langley under NASA Contract NAG-1-448 with Dr. Brian J. Jensen as the contract monitor. We are grateful to professor Chrys Wesdemiotis (Department of Chemistry, The University of Akron) for MALDI–TOF analysis and detailed peak assignment.

References and Notes

(1) (a) Baek, J.-B.; Harris, F. W. *Macromolecules* **2005**, *38*, 297. (b) Baek, J.-B.; Harris, F. W. *Polym. Prepr.* **2000**, *41* (*1*), 157. (c) Baek, J.-B.; Harris, F. W. *J. Polym. Sci., Part A: Polym. Chem.* **2005**, *43*, 78.

(2) Hergenrother, P. M. *J. Polym. Sci., Part A1* **1968**, *6*, 3170.

(3) (a) Kraft, A.; Grimsdale, A. C.; Holmes, A. B. *Angew. Chem., Int. Ed.* **1998**, *37*, 402 and references therein. (b) Lee, B. L.; Yamamoto, T. *Macromolecules* **1999**, *32*, 1375. (c) Baek, J.-B.; Chien, L.-C. *Polym. Prepr.* **1999**, *40*(2), 607. (d) Cui, Y.; Zhang, X.; Jenekhe, S. A. *Macromolecules* **1999**, *32*, 3824. (e) Justin Thomas, K. R.; Lin, J. T.; Tao, Y. T.; Chuen, C.-H. *Chem. Mater.* **2002**, *14*, 2796. (f) Thlelakkat, M. M.; Posch, P.; Schmidt, H.-W. *Macromolecules* **2001**, *34*, 7441. (g) Jonforsen, M.; Johansson, T.; Inganäs, O.; Andersson, M. R. *Macromolecules* **2002**, *35*, 1638. (h) Zhan, X.; Liu, Y.; Wu, X.; Wang, S.; Zhu, D. *Macromolecules* **2002**, *35*, 2529. (i) Bangcuyo, C. G.; Ellsworth, J. M.; Evans, U.; Myrick, M. L.; Bunz, U. H. F. *Macromolecules* **2003**, *36*, 546.

(4) (a) Harris, F. W.; Korleski, J. E. *Polym. Mater. Sci. Eng.* **1989**, *61*, 870. (b) Harris, F. W.; Korleski, J. E. US Patent 5,030,-704, 1991. (c) Kim, B. S.; Korleski, J. E.; Zhang, Y.; Klein, D. J.; Harris, F. W. *Polymer* **1999**, *40*, 4553. (d) Baek, J.-B.; Harris, F. W. *Polym. Prepr.* **1999**, *40* (2), 882. (e) Klein, D. J.; Baek, J.-B.; Harris, F. W. *Polym. Prepr.* **1999**, *40* (2), 886. (f) Ooi, I. H.; Hergenrother, P. M.; Harris, F. W. *Polymer* **2000**, *41*, 5095. (g) Klein, D. J.; Modarelli, D. A.; Harris, F. W. *Macromolecules* **2001**, *34*, 2427. (h) Baek, J.-B.; Harris, F. W. *J. Polym. Sci., Part A: Polym. Chem.* **2004**, *42*, 6318.

(5) (a) Baek, J.-B.; Harris, F. W. *Polym. Prepr.* **2001**, *42* (1), 566. (b) Baek, J.-B.; Harris, F. W. *J. Polym. Sci., Part A: Polym. Chem.* **2005**, *43*, 801.

(6) Srinivasan, S.; Twieg, R.; Hedrick, J. L.; Hawker, C. J. *Macromolecules* **1996**, *29*, 8543.

(7) (a) Markoski, L. J.; Moore, J. S.; Sendijarevic, I.; McHugh, A. J. *Macromolecules* **2001**, *34*, 2695. (b) Jikei, M.; Fujii, K.; Yang, G.; Kakimoto, M. *Macromolecules* **2000**, *33*, 6228. (c) Baek, J.-B.; Tan, L.-S. *Polymer* **2003**, *34*, 3451.

(8) Loewe, H.; Urbanietz, J.; Kirsch, R.; Duewel, D. Ger. Offen., DE 2,443,297, 1985.

(9) Seko, N.; Yoshino, K.; Yokota, K.; Tsukamoto, G. *Chem. Pharm. Bull.* **1991**, *39*, 651.

(10) For reviews of hyperbranched polymers, see: (a) Jikei, M.; Kakimoto, M. *Prog. Polym. Sci.* **2001**, *26*, 1233. (b) Voit, B. *J. Polym. Sci., Part A: Polym. Chem.* **2000**, *36*, 2505. (c) Frey, H. *Angew. Chem., Int. Ed. Engl.* **1999**, *2193*, 3. (d) Hult, A.; Johansson, M.; Malmström, E. *Adv. Polym. Sci.* **1999**, *143*, 1. (e) Hawker, C. J. *Adv. Polym. Sci.* **1999**, 113–160. (f) Kim, Y. H. *J. Polym. Sci., Part A: Polym. Chem.* **1998**, *36*, 1685. (g) Malmstrom, E.; Hult, A. *J. Macromol. Sci.—Rev. Macromol. Chem. Phys.* **1997**, *37*, 555. (h) Fréchet, J. M. J.; Hawker, C. J.; Gitsov, I.; Leon, J. W. *J. Macromol. Sci Pure Appl. Chem.* **1996**, *A33*, 1399. (i) Voit, B. I. *Acta Polym.* **1995**, *46*, 87. (j) Fréchet, J. M. J. *J. Macromol. Sci. Pure Appl. Chem.* **1996**, *A33*, 1399.

(11) (a) Kim, Y. H.; Webster, O. W. *Polym. Prepr.* **1988**, *29* (2), 310. (b) Kim, Y. H.; Webster, O. W. *J. Am. Chem. Soc.* **1990**, *112*, 4592.

(12) (a) de Brabender-van den Berg, E. M. M.; Meijer, E. W. *Angew. Chem., Int. Ed. Engl.* **1993**, *32*, 1308. (b) Turner, S. R.; Voit, B. I.; Mourey, T. H. *Macromolecules* **1993**, *26*, 4617. (c) Turner, S. R.; Walter, F.; Voit, B. I.; Mourey, T. H. *Macromolecules* **1994**, *27*, 1611. (d) Wooley, K. L.; Hawker, C. J.; Pochan, J. M.; Fréchet, J. M. J. *Macromolecules* **1993**, *26*, 1514. (e) Kim, Y. H.; Beckenbauer, R. *Macromolecules* **1994**, *27*, 1968.

(13) (a) Tomalia, D. A.; Durst, H. D. *Top. Curr. Chem.* **1993**, *165*, 194. (b) Young, J. K.; Baker, G. R.; Newkome, G. R.; Morris, K. F.; Johnson Jr. C. S. *Macromolecules* **1994**, *27*, 3464.

(14) (a) Kraft, A.; Grimsdale, A. C.; Holmes, A. B. *Angew. Chem., Int. Ed.* **1998**, *37*, 402 and references therein; (b) Lee, B. L.; Yamamoto, T. *Macromolecules* **1999**, *32*, 1375. (c) Baek, J.-B.; Chien, L.-C. *Polym. Prepr.* **1999**, *40* (2), 607. (d) Baek, J.-B.; Chien, L.-C. *J. Polym. Sci., Part A: Polym. Chem.* **2004**, *42*, 3587. (e) Cui, Y.; Zhang, X.; Jenekhe, S. A. *Macromolecules* **1999**, *32*, 3824. (f) Justin Thomas, K. R.; Lin, J. T.; Tao, Y. T.; Chuen, C.-H. *Chem. Mater.* **2002**, *14*, 2796. (g) Thlelakkat, M. M.; Posch, P.; Schmidt, H.-W. *Macromolecules* **2001**, *34*, 7441. (h) Jonforsen, M.; Johansson, T.; Inganäs, O.; Andersson, M. R. *Macromolecules* **2002**, *35*, 1638. (i) Zhan, X.; Liu, Y.; Wu, X.; Wang, S.; Zhu, D. *Macromolecules* **2002**, *35*, 2529. (j) Bangcuyo, C. G.; Ellsworth, J. M.; Evans, U.; Myrick, M. L.; Bunz, U. H. F. *Macromolecules* **2003**, *36*, 546.

MA048338R